

**Supported, Alkali-Promoted Cobalt Oxide Catalysts for NO<sub>x</sub> Removal from Coal  
Combustion Flue Gases**

Final Report

September 15, 2004  
December 31, 2005

Morris D. Argyle

March 2006

DE-FG26-04NT42181

University of Wyoming  
Department of Chemical and Petroleum Engineering  
1000 E. University Ave.  
Department 3295  
Laramie, WY 82071

**DISCLAIMER:**

This report was prepared as an account of work sponsored by an agency of the United States Government. Neither the United States Government nor any agency thereof, nor any of their employees, makes any warranty, express or implied, or assumes any legal liability or responsibility for the accuracy, completeness, or usefulness of any information, apparatus, product, or process disclosed, or represents that its use would not infringe privately owned rights. Reference herein to any specific commercial product, process, or service by trade name, trademark, manufacturer or otherwise does not necessarily constitute or imply its endorsement, recommendation, or favoring by the United States Government or any agency thereof. The views and opinions of authors expressed herein do not necessarily state or reflect those of the United States Government or any agency thereof.

## ABSTRACT

A series of cobalt oxide catalysts supported on alumina ( $\gamma$ - $\text{Al}_2\text{O}_3$ ) were synthesized with varying contents of cobalt and of added alkali metals, including lithium, sodium, potassium, rubidium, and cesium. Unsupported cobalt oxide catalysts and several cobalt oxide catalysts supported ceria ( $\text{CeO}_2$ ) with varying contents of cobalt with added potassium were also prepared. The catalysts were characterized with UV-visible spectroscopy and were examined for  $\text{NO}_x$  decomposition activity. The  $\text{CoO}_x/\text{Al}_2\text{O}_3$  catalysts and particularly the  $\text{CoO}_x/\text{CeO}_2$  catalysts show  $\text{N}_2\text{O}$  decomposition activity, but none of the catalysts (unsupported  $\text{Co}_3\text{O}_4$  or those supported on ceria or alumina) displayed significant, sustained NO decomposition activity. For the  $\text{Al}_2\text{O}_3$ -supported catalysts,  $\text{N}_2\text{O}$  decomposition activity was observed over a range of reaction temperatures beginning about 723 K, but significant (>50%) conversions of  $\text{N}_2\text{O}$  were observed only for reaction temperatures >900 K, which are too high for practical commercial use. However, the  $\text{CeO}_2$ -supported catalysts display  $\text{N}_2\text{O}$  decomposition rates similar to the  $\text{Al}_2\text{O}_3$ -supported catalysts at much lower reaction temperatures, with activity beginning at ~573 K. Conversions of >90% were achieved at 773 K for the best catalysts. Catalytic rates per cobalt atom increased with decreasing cobalt content, which corresponds to increasing edge energies obtained from the UV-visible spectra. The decrease in edge energies suggests that the size and dimensionality of the cobalt oxide surface domains increase with increasing cobalt oxide content. The rate data normalized per mass of catalyst that shows the activity of the  $\text{CeO}_2$ -supported catalysts increases with increasing cobalt oxide content. The combination of these data suggest that supported cobalt oxide species similar to bulk  $\text{Co}_3\text{O}_4$  are inherently more active than more dispersed cobalt oxide species, but this effect was only observed with the  $\text{CeO}_2$ -supported catalysts.

## TABLE OF CONTENTS

INTRODUCTION	1
EXECUTIVE SUMMARY	4
EXPERIMENTAL	6
RESULTS AND DISCUSSION	8
CONCLUSION	24
REFERENCES	26

## LIST OF GRAPHICAL MATERIALS

### FIGURES

Figure 1: NO conversion of several direct NO <sub>x</sub> decomposition catalysts in the absence and in the presence of oxygen.	2
Figure 2: UV-visible spectra for a series of 0.035 Rb-CoO <sub>x</sub> /Al <sub>2</sub> O <sub>3</sub> catalysts.	8
Figure 3: UV-visible spectra for a series of 0.035 K-CoO <sub>x</sub> /CeO <sub>2</sub> catalysts, as well as for unsupported 0.035 K-Co <sub>3</sub> O <sub>4</sub> and CeO <sub>2</sub> .	9
Figure 4: UV-visible absorption edge energies for the series of 0.035 Rb-CoO <sub>x</sub> /Al <sub>2</sub> O <sub>3</sub> catalysts and the series of 0.035 K-CoO <sub>x</sub> /CeO <sub>2</sub> catalysts.	11
Figure 5: N <sub>2</sub> O conversion as a function of reaction temperature for a series of CoO <sub>x</sub> /CeO <sub>2</sub> catalysts with 0.035 K:Co.	14
Figure 6: N <sub>2</sub> O decomposition rate per mass of catalyst as a function of reaction temperature for a series of CoO <sub>x</sub> /CeO <sub>2</sub> catalyst with 0.035 K:Co atomic ratios.	15
Figure 7: N <sub>2</sub> O conversion as a function of reaction temperature for a series of 0.035 K-CoO <sub>x</sub> /Al <sub>2</sub> O <sub>3</sub> catalysts with varying amounts of Co.	17
Figure 8: N <sub>2</sub> O conversion per mass of catalyst as a function of reaction temperature for a series of CoO <sub>x</sub> /CeO <sub>2</sub> and CoO <sub>x</sub> /Al <sub>2</sub> O <sub>3</sub> catalysts with 0.035 K:Co atomic ratios.	18
Figure 9: N <sub>2</sub> O decomposition rate normalized per mole of Co as a function of reaction temperature for the series of (a) CoO <sub>x</sub> /CeO <sub>2</sub> catalysts and (b) CoO <sub>x</sub> /Al <sub>2</sub> O <sub>3</sub> catalysts with 0.035 K:Co atomic ratios.	19
Figure 10: N <sub>2</sub> O decomposition rate normalized per weight of catalyst as a function of reaction temperature for a 3.4 wt% CoO <sub>x</sub> /Al <sub>2</sub> O <sub>3</sub> catalyst with varying amounts of potassium.	23

### TABLES

Table 1: N <sub>2</sub> O conversion rates normalized per mass of catalyst and for Co content for alumina-supported catalysts.	21
Table 2: N <sub>2</sub> O conversion rates normalized per mass of catalyst and for Co content for ceria-supported catalysts.	21
Table 3: N <sub>2</sub> O conversion rates normalized per mass of catalyst and for Co content for the 2.5 wt% Co/Al <sub>2</sub> O <sub>3</sub> (3.4 wt% CoO <sub>x</sub> /Al <sub>2</sub> O <sub>3</sub> ) catalysts showing typical effects of K addition.	24

## INTRODUCTION

The production of various oxides of nitrogen ( $\text{NO}_x$ ) in combustion processes is a serious environmental problem that contributes to photochemical smog, ozone depletion, greenhouse gas formation, and acid rain [1-2]. Elimination of  $\text{NO}_x$  through selective catalytic reduction (SCR) using amine-based reductants (typically ammonia) and vanadia catalysts supported on titania is an established process that is currently used industrially [3-4]. The existing process has several drawbacks, including the requirement of an expensive reductant that is difficult to precisely dose, which can lead to ammonia break-through (slip) with associated negative environmental impacts, and the requirement of most current catalysts to operate in a narrow temperature range that leads to energy inefficiencies and retrofit difficulties for proper placement of the catalyst bed. Applying current SCR technology to coal combustion flue gases is further complicated by the fine particulates that escape the fly ash recovery processes and the potential for catalyst poisoning from arsenic and mercury. Therefore, new SCR catalysts are required that can operate either using other reductants present in the flue gas (e.g., carbon monoxide) or without reductants through direct  $\text{NO}_x$  decomposition. Catalysts active over a wider range of temperatures under the harsh conditions in coal combustion flue gases are also needed.

Three-way automotive catalytic converters, which incorporate rhodium with platinum and various metal oxides in the catalysts, provide an example of non-amine based reductants because they use unburned hydrocarbons and CO to effectively reduce  $\text{NO}_x$  emissions [5]. Supported precious metals can also directly decompose  $\text{NO}_x$  [6-7]. Unfortunately, these expensive precious metals are unlikely to be cost effective for industrial use and probably would not remain active as a result of poisoning from sulfur and heavy metals present in the coal flue

gas. Therefore, novel catalysts are desired that can directly decompose  $\text{NO}_x$  to  $\text{N}_2$  and  $\text{O}_2$  while withstanding the severe operating conditions of coal combustion flue gases.

This goal of this project was to develop a catalyst for the direct decomposition of  $\text{NO}_x$ , building on recently published work on the activity of alkali-promoted cobalt oxide ( $\text{A}_x\text{Co}_3\text{O}_4$ , where A is any alkali metal) in the direct decomposition of  $\text{NO}_x$  [8].  $\text{Co}_3\text{O}_4$  was shown to directly decompose  $\text{NO}_x$  several decades ago [9], but only recently has the activity been shown to depend on incorporation of an alkali metal promoter [8]. Haneda *et al.* also showed that these catalysts retain a significant portion (>50%) of their activity in the presence of oxygen, while other direct NO decomposition catalysts, such as zeolites containing copper (e.g. Cu-ZSM-5) and supported precious metals (e.g., palladium supported on  $\text{Al}_2\text{O}_3$ ) lose the majority of their activity in the presence of as little as 1%  $\text{O}_2$ , as shown in Figure 1 [8].

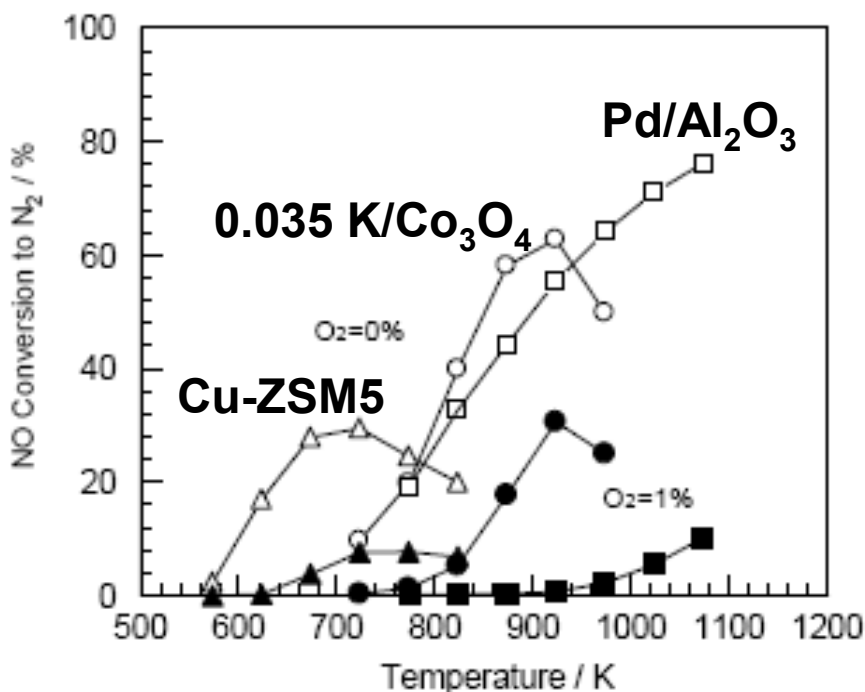


**Figure 1.** NO conversion of an unsupported 0.035 K -  $\text{Co}_3\text{O}_4$  catalyst (circles) compared with two other direct  $\text{NO}_x$  decomposition catalysts, Cu-ZSM5 (triangles) and supported palladium (squares) [8]. The open symbols are for reactions in the absence of  $\text{O}_2$ , while the filled symbols are for reaction in the presence of 1%  $\text{O}_2$ .

The work of Haneda *et al.* involved unsupported, alkali-doped  $\text{Co}_3\text{O}_4$  of low surface area ( $\sim 25 \text{ m}^2/\text{g}$ ) [8]. The present project used supported  $\text{A}_x\text{Co}_3\text{O}_4$  on  $\gamma\text{-Al}_2\text{O}_3$  and  $\text{CeO}_2$  in an attempt to enhance activity for  $\text{NO}_x$  decomposition. Two series of catalysts with different concentrations of the active metal oxide were synthesized in an attempt to produce a variety of surface species with different surface cobalt oxide domain sizes, ranging from isolated cobalt oxide structures to two-dimensional layers on the support to three-dimensional structures similar to crystalline  $\text{Co}_3\text{O}_4$ . These catalysts were tested to determine their effectiveness for both  $\text{NO}$  and  $\text{N}_2\text{O}$  decomposition at typical coal combustion flue gas temperatures.

## EXECUTIVE SUMMARY

This project was part of a research effort aimed at development of advanced selective catalytic reduction (SCR) catalysts to reduce emissions of nitrogen oxides ( $\text{NO}_x$ ) from coal combustors. Traditional SCR systems inject a reductant, such as ammonia or hydrocarbons, into the flue gas to be treated and then pass the mixture over a catalyst bed to form elemental nitrogen ( $\text{N}_2$ ) and oxygen ( $\text{O}_2$ ), along with thermodynamically stable compounds such as water or carbon dioxide. The focus of this research was to develop catalysts that can directly decompose  $\text{NO}_x$  compounds into  $\text{N}_2$  and  $\text{O}_2$ , without the need for an added reductant. These reductants add both to the cost of SCR operation and can exacerbate environmental impacts if too much is added and the unreacted amount escapes to the atmosphere.

Previously published research reported that cobalt oxide catalysts with added alkali metals were effective nitric oxide (NO) decomposition catalysts. Further, these catalysts maintained their activity in the presence of concentrations of  $\text{O}_2$  that are found in coal combustion flue gases. This ability has not been observed in other direct NO decomposition catalysts, such as supported palladium or zeolites containing copper (e.g., Cu-ZSM5). The hypothesis of this research was that the catalytic properties of the alkali-cobalt oxide could be enhanced by supporting it on another metal oxide, such as alumina or ceria.

During this study, a catalytic microreactor was constructed and over 100 catalysts were synthesized, including catalysts supported on  $\gamma\text{-Al}_2\text{O}_3$  with varying content of cobalt oxides and five alkali oxides,  $\text{CeO}_2$ -supported catalysts with several cobalt oxide contents with added potassium, and unsupported cobalt oxide ( $\text{Co}_3\text{O}_4$ ) with and without added potassium. A representative subset of these catalysts was characterized using UV-visible spectroscopy. Kinetic experiments were performed with both nitric oxide (NO) and nitrous oxide ( $\text{N}_2\text{O}$ ) as the reactants. A mass spectrometer (MS) procured as part of the project was used to collect the data from the kinetic experiments.

The kinetic experiments reveal that the catalysts are effective at decomposing  $\text{N}_2\text{O}$ , but show no steady-state activity for NO decomposition. Rates of  $\text{N}_2\text{O}$  decomposition per cobalt atom increased with decreasing cobalt oxide content, which corresponds to decreasing size and dimensionality of the cobalt oxide surface domains, as suggested by the UV-visible spectra. However, the ceria-supported catalysts that produce the highest rates of  $\text{N}_2\text{O}$  decomposition, normalized per mass of catalyst, generally have higher cobalt oxide contents, suggesting that the fewer exposed surface cobalt oxides in larger three-dimensional domains may be more reducible and may be better able to participate in catalytic turnovers. The effect of the ceria support is significant and the supported catalysts are 2-3 times more active per mass of catalyst and 20-200 times more active per cobalt atom compared to unsupported  $\text{Co}_3\text{O}_4$ . A portion of this activity is due to the ceria support itself, but the combined effect of the cobalt oxide and ceria is larger than either individual component. The alumina support does not increase rates normalized per mass of catalyst. Coincidentally, rates per mass of catalyst are approximately the same at a given reaction temperature for all of the alumina-supported catalysts, unsupported  $\text{Co}_3\text{O}_4$ , and ceria with no cobalt; and all of these rates are 2-3 times lower than those found for the ceria-supported catalysts with similar cobalt oxide content. A literature account reported that alkali metal oxides enhanced reaction rates for direct NO decomposition, but this effect was not observed for  $\text{N}_2\text{O}$  decomposition. In fact, alkali oxide additions decrease  $\text{N}_2\text{O}$  decomposition rates. The decrease in rates is correlated to the amount of alkali addition.



The ceria-supported catalysts work well for  $\text{N}_2\text{O}$  decomposition. Their operating temperatures ( $<650\text{K}$ ) are sufficiently low that they might be considered for use in certain industrial operations.

Future work may include testing other catalyst compositions with molybdena, tungsten oxide, iron oxide, and/or nickel oxide to investigate if further improvements in performance are obtainable while improving the sulfur tolerance and hydrothermal stability of the catalysts in actual coal combustion flue gases. In addition, development of better catalysts that produce  $\text{N}_2\text{O}$  from  $\text{NO}$  would allow them to be placed upstream of the  $\text{N}_2\text{O}$  decomposition catalysts developed in this study. Thus, both  $\text{NO}$  and  $\text{N}_2\text{O}$  could be directly decomposed by first converting the  $\text{NO}$  to  $\text{N}_2\text{O}$  and then decomposing the  $\text{N}_2\text{O}$ .

## EXPERIMENTAL

Three types of cobalt oxide catalysts were synthesized. First, a series of cobalt oxide catalysts with alkali metals supported on  $\gamma$ -alumina ( $\gamma$ -Al<sub>2</sub>O<sub>3</sub>) were prepared by incipient wetness impregnation. Appropriate amounts of cobalt (II) nitrate hexahydrate (Co(NO<sub>3</sub>)<sub>2</sub>·6H<sub>2</sub>O, Acros, 99%), lithium nitrate (LiNO<sub>3</sub>, Alfa Aesar, 99.999%), sodium nitrate (NaNO<sub>3</sub>, Alfa Aesar, 99.999%), potassium nitrate (KNO<sub>3</sub>, Alfa Aesar, 99.994%), rubidium nitrate (RbNO<sub>3</sub>, Alfa Aesar, 99.975%), and cesium nitrate (CsNO<sub>3</sub>, Alfa Aesar, 99.99%) were dissolved in ~10 ml of deionized water and mixed with appropriate amounts of  $\gamma$ -alumina ( $\gamma$ -Al<sub>2</sub>O<sub>3</sub>, Alfa Aesar high surface area, ~220 m<sup>2</sup>/g) to form a thick paste. The cobalt content of each catalyst was varied from 1.0, 2.5, 5.0, 7.5, 10 and 15 wt% Co (equivalent to 1.3, 3.4, 6.8, 10.2, 13.6, and 20.4 nominal wt% Co<sub>3</sub>O<sub>4</sub>). For each cobalt content, alkali metals were added in 0.01, 0.035, or 0.05 alkali:cobalt atomic ratios. In this manner, 96 catalysts supported on alumina were synthesized. The catalysts were dried overnight at 90°C and calcined in flowing dry air for 3 h at 500°C. Second, a catalyst duplicating the unsupported catalysts reported by Haneda *et al.* [8], with a nominal composition of 0.035 atom ratio of potassium to cobalt (K:Co), was produced by dissolving an appropriate amount of cobalt nitrate in ~10 ml of deionized water. The solution was then titrated using ammonium carbonate ((NH<sub>4</sub>)<sub>2</sub>CO<sub>3</sub>, Baker reagent grade) to a pH of approximately 8. The resulting gel was washed with deionized water, dried overnight at 90°C, and calcined in flowing dry air for 3 h at 550°C. Potassium nitrate was dissolved in deionized water and impregnated into the Co<sub>3</sub>O<sub>4</sub> followed by calcination in flowing dry air for 3 h at 700°C. Finally, a second series of supported cobalt oxide catalysts was produced by coprecipitation of cerium (III) nitrate (Ce(NO<sub>3</sub>)<sub>3</sub>, Aldrich, 99.99%) with appropriate amounts of the cobalt nitrate in ~50 ml of deionized water. The solution was then titrated using ammonium

carbonate ( $(\text{NH}_4)_2\text{CO}_3$ , Baker reagent grade) to a pH of approximately 8. The resulting gel was washed with deionized water, dried overnight at  $90^\circ\text{C}$ , and calcined in flowing dry air for 3 h at  $550^\circ\text{C}$ . Potassium nitrate was dissolved in deionized water and impregnated into the  $\text{CoO}_x/\text{CeO}_2$  catalysts at 0.035 K:Co ratios, followed by calcination in flowing dry air for 3 h at  $700^\circ\text{C}$ . The Co content of the ceria-supported catalysts was varied from 0.73, 1.8, 3.6, and 11 wt% Co (equivalent to 1.0, 2.5, 5.0 and 15 nominal wt%  $\text{Co}_3\text{O}_4$ ). 5 g of each of the catalysts were made.

The catalysts were characterized using ultraviolet (UV)-visible spectroscopy (Cary 4000 Spectrophotometer fitted with a Harrick Praying Mantis diffuse reflectance attachment). The catalysts were dehydrated at  $450^\circ\text{C}$  in flowing 5% oxygen ( $\text{O}_2$ ), 95% argon (Ar). Spectra of the dehydrated catalysts were obtained at room temperature over an energy range of  $\sim 1.5$  eV to 6.2 eV in 0.0012 eV steps.

The catalysts were tested in a flow microreactor, with approximately 0.04 g of catalyst placed in a U-tube quartz reactor and heated to the reaction temperature in a furnace. Prior to reaction, the catalysts were treated for 1 h in 5%  $\text{O}_2$  in balance Ar (Airgas) at the highest temperature of the planned experiments to dehydrate and thermally stabilize them. Mass flow controllers maintained the reactant flow through the reactor at  $0.5\text{ cm}^3/\text{s}$  of 987 ppm nitric oxide (NO) with 1% Ar in balance helium (He) (Airgas) for the NO decomposition experiments. For the  $\text{N}_2\text{O}$  decomposition experiments, 995 ppm nitrous oxide ( $\text{N}_2\text{O}$ ) in balance nitrogen (Airgas) was mixed with Ar as an internal standard to produce a total flowrate of  $0.6\text{ cm}^3/\text{s}$  with 818 ppm  $\text{N}_2\text{O}$ . Reactor temperatures were varied between 573 K and 1023 K in 50 K increments. The reaction progress was monitored in real time using a quadrupole mass spectrometer (MKS Cirrus 100). Blank experiments (without catalyst) at the highest reactor temperature used in this study (1023 K) did not produce measurable conversion of either NO or  $\text{N}_2\text{O}$ .

## RESULTS AND DISCUSSION

### UV-visible Spectra

The UV-visible spectra collected for one representative series of  $\text{CoO}_x/\text{Al}_2\text{O}_3$  catalysts with 0.035 Rb:Co are shown in Figure 2 and for the series of  $\text{CoO}_x/\text{CeO}_2$  catalysts with 0.035 K:Co are shown in Figure 3. The ordinate in these plots is the square root of the product of the photon energy and the Kubelka-Munk function ( $F(R)$ ), which is the ratio of the absorbance and scattering parameters for the catalyst samples. Thus, the y-axis is a measure of absorbance of the catalyst samples. The spectra in Figure 2 show that absorbance increases with increasing cobalt

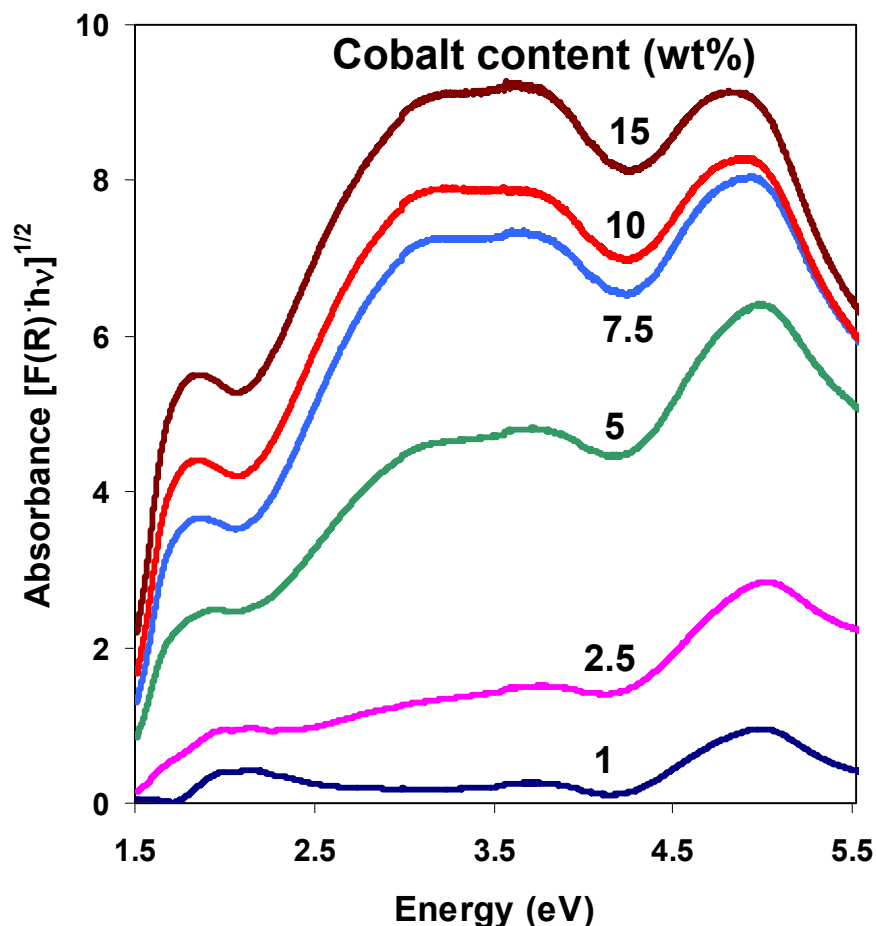


**Figure 2.** UV-visible spectra for the series of 0.035 Rb- $\text{CoO}_x/\text{Al}_2\text{O}_3$  catalysts. The spectra were obtained at room temperature after dehydration in flowing 5%  $\text{O}_2/\text{Ar}$  ( $0.5 \text{ cm}^3/\text{s}$ ) at 723 K.

content of the alumina-supported catalysts across the energy range studied. In the visible region, this data are consistent with the range of observed colors of the catalysts, which progress from white or light pink for the 1 wt% Co catalyst through gray and then black for the 15 wt% Co catalyst. The other alumina-supported catalysts with other alkali oxides have similar physical appearances and similar UV-visible spectra. In contrast, the ceria supported catalysts do not increase monotonically in the visible region. However, the color of these catalysts vary from yellow for the ceria to gray to black with increasing cobalt content in a manner similar to the

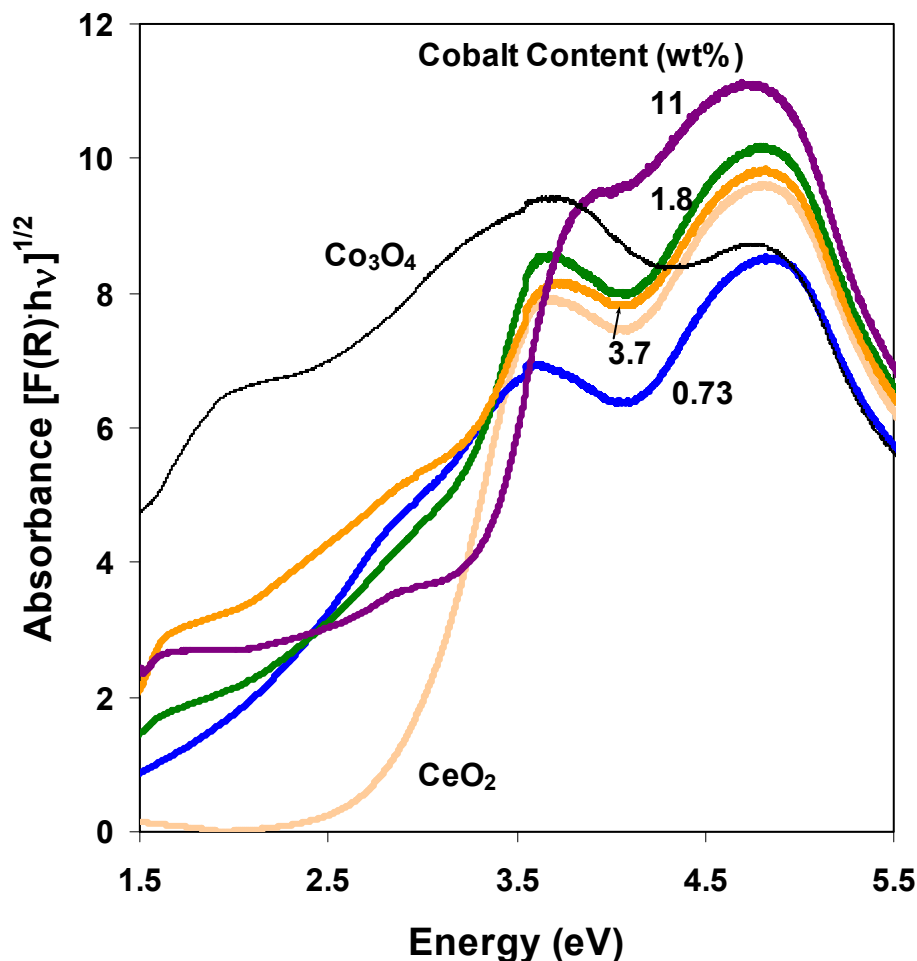


**Figure 3.** UV-visible spectra for the series of  $0.035 \text{ K-CoO}_x/\text{CeO}_2$  catalysts, as well as for unsupported  $0.035 \text{ K-Co}_3\text{O}_4$  and  $\text{CeO}_2$ . The spectra were obtained at room temperature after dehydration in flowing 5%  $\text{O}_2/\text{Ar}$  ( $0.5 \text{ cm}^3/\text{s}$ ) at 723 K.

alumina-supported catalysts. The more complex spectra of the ceria-supported catalysts (Figure 3), compared to the spectra of the alumina-supported catalysts (Figure 2), suggests more complex interactions with the ceria support. As will be discussed below, these more complex interactions appear to be related to the higher rates of  $\text{N}_2\text{O}$  decomposition for the ceria-supported catalysts.

The wide absorption bands centered around 1.9 eV and 3.5 eV in both Figures 2 and 3 have been attributed to ligand to metal charge transfer (LMCT) electronic transitions between O and Co [10, 11]. The higher energy band near 5 eV has not been described in these literature references, but is most likely associated with the presence of the Co, as shown by the increasing intensity of this band with increasing Co content and the similarity of the shape and position of the  $\text{Co}_3\text{O}_4$  band (Figure 3).

The absorption edge energy for each of these catalysts based on this high energy band is shown in Figure 4. One definition for the edge energy is the intersection of a line extrapolated from the linear portion of the rising absorption band and the x-axis, which corresponds to the beginning of the absorption band when photons start to be absorbed by the catalyst samples. The edge energy decreases with increasing cobalt content, which is consistent with increasing size of cobalt oxide domains that are similar to three-dimensional crystalline  $\text{Co}_3\text{O}_4$  structures. The measured edge energy for the 0.035 K- $\text{Co}_3\text{O}_4$  sample is low ( $\sim 0.5$  eV), but this value is probably influenced by the shoulder of the wide LMCT band. A published value for unsupported  $\text{Co}_3\text{O}_4$  edge energy has not been found for comparison with our measured value, but based on analogy with supported and unsupported  $\text{V}_2\text{O}_5$  catalysts [12], the edge energy of the 15 wt% Co/ $\text{Al}_2\text{O}_3$  or  $\text{CoO}_x/\text{CeO}_2$  catalysts ( $\sim 1.4$  eV) are probably similar to the edge energy of unsupported  $\text{Co}_3\text{O}_4$ . Edge energy has previously been shown to correlate with catalytic activity [12].

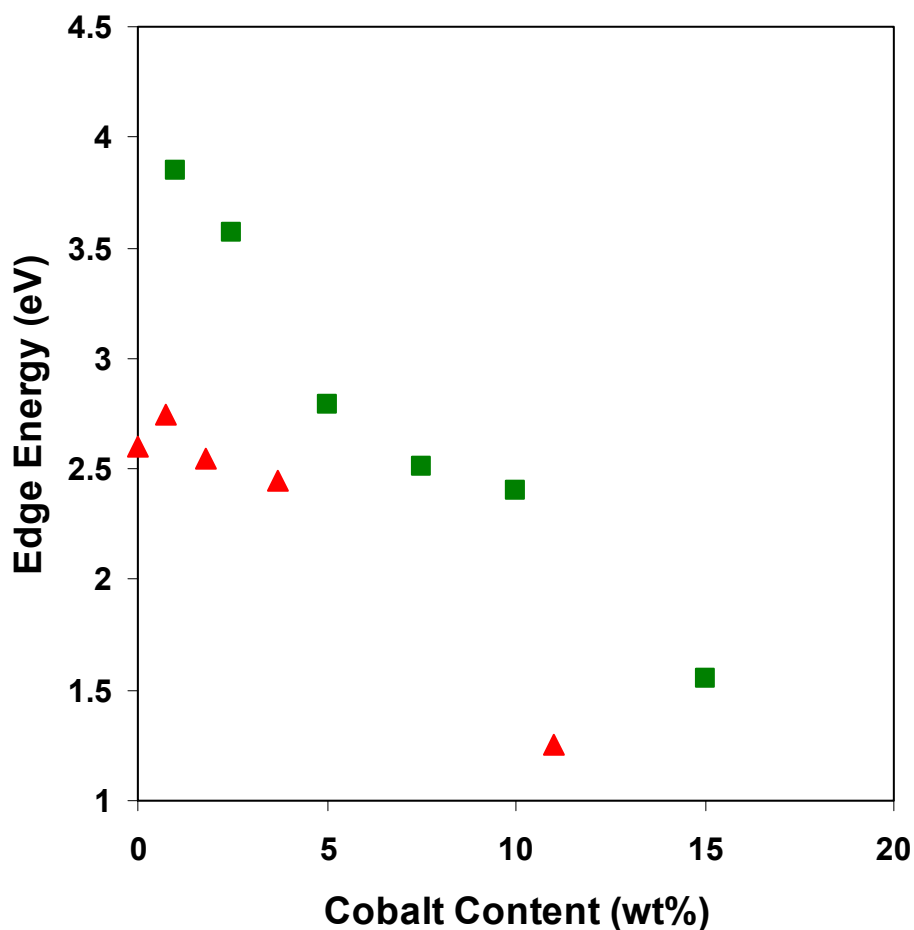


**Figure 4.** UV-visible absorption edge energies for the series of 0.035 Rb-CoO<sub>x</sub>/Al<sub>2</sub>O<sub>3</sub> catalysts (squares) and 0.035 K-CoO<sub>x</sub>/CeO<sub>2</sub> catalysts (triangles).

### NO Decomposition

Virtually no steady state decomposition of NO was observed for the CoO<sub>x</sub>/Al<sub>2</sub>O<sub>3</sub> catalysts. Observed NO conversions were never more than 10%, even at reaction temperatures as high as 1023 K, and these conversions were not sustained. Transient activity was observed following step changes in reaction temperature, but the transient O<sub>2</sub> production appeared to be merely the desorption of adsorbed species that accumulated at each reaction temperature step. At higher reaction temperatures (>973 K), the O<sub>2</sub> product displayed the largest transient and

required the most time (~1 h) to approach the steady state value. However, the rate of O<sub>2</sub> production decreased back to the baseline value, which indicates that the effect was not catalytic. No N<sub>2</sub> product was detected in conjunction with the O<sub>2</sub> production, suggesting that the nitrogen formed a nitride compound with the cobalt or alumina.

The failure of the alumina-supported catalysts led us to attempt to reproduce the results reported in the literature by Haneda *et al.* for their unsupported ACo<sub>3</sub>O<sub>4</sub> catalysts, where A is an alkali metal. We were unable to duplicate their results. Our catalysts synthesized in a similar manner to the ones produced by Haneda *et al.* [8] again showed insignificant NO decomposition activity. We were unable to reconcile these results with the work of Haneda *et al.* However, we are confident that our data showing no NO activity are correct. Some unidentified difference in the synthesis procedure may explain the differences in activity, but another consideration is the Haneda *et al.* paper appears to contain errors because the reported activity exceeds the amount of NO reactant fed to the reactor.

Due to the unsatisfactory results of both the bulk oxide prepared by co-precipitation and cobalt oxide catalysts prepared by incipient wetness impregnation of  $\gamma$ -Al<sub>2</sub>O<sub>3</sub>, we synthesized several catalysts by co-precipitation with ceria (CeO<sub>2</sub>) to test a second support prepared by a different technique. Catalysts with atomic ratios of K:Co of 0.035 and 1 to 15 wt% Co were prepared with ceria. The resulting catalysts were somewhat more active than the catalysts supported on alumina, but still showed insignificant NO decomposition activity (again, transient activity with less than 10% conversion). The oxygen transients were larger than for the CoO<sub>x</sub>/Al<sub>2</sub>O<sub>3</sub> catalysts. Some sustained activity appeared at reaction temperatures above 923 K, but the NO conversion was still only about 5% (based on N<sub>2</sub> formation). In this case, N<sub>2</sub> was detected, but a material balance showed that the amount of O<sub>2</sub> formed was greater than the rate



produced by NO decomposition. This result can be explained by oxygen release from the catalyst or support lattice atoms, which is a form of autoreduction that would be consistent with the oxygen storage and release ability of ceria. Thus, the majority of the apparent sustained “activity” at 973 K was a loss of oxygen from the catalyst instead of from NO decomposition.

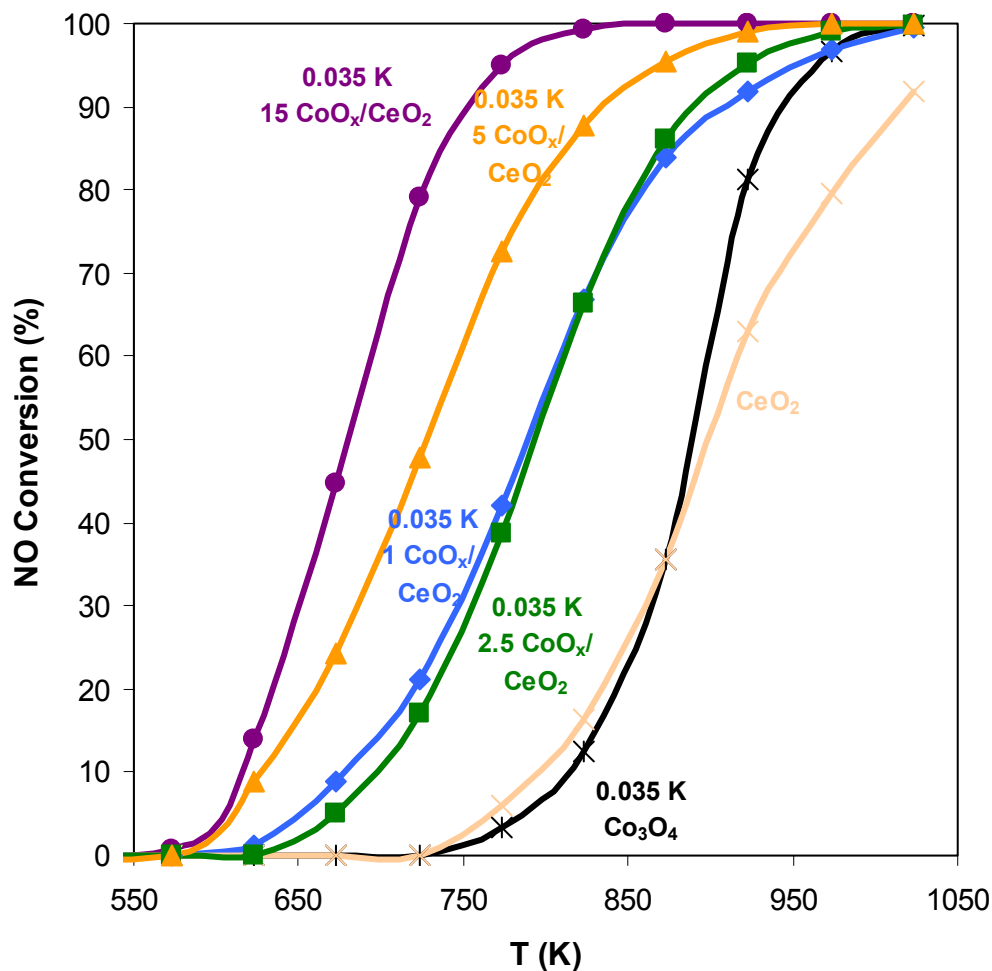
Ceria was chosen as a support because of its ability to act as an oxygen storage and release support, which makes it an important component of automobile catalytic converters [5, 13]. A similar series of  $\text{CoO}_x/\text{CeO}_2$  catalysts had also been shown to be effective CO oxidation catalysts [14, 15]. As we had originally been concerned about the catalyst ability to exchange and desorb oxygen, ceria seemed like a good support candidate. Unfortunately, our data suggest that nitrogen recombination is the more difficult step. While ceria is better for nitrogen recombination than alumina because some  $\text{N}_2$  was formed, detectable  $\text{N}_2$  is formed only at very high reaction temperatures (above 923 K), either because the N atoms do not desorb or a nitride compound is stable at lower reaction temperatures, as was suggested for the alumina catalysts.

At higher reaction temperatures (above ~950 K) during the NO (and  $\text{N}_2\text{O}$ ) decomposition experiments, the alumina-supported catalysts turned a pale blue color, which suggests the formation of an aluminate structure with the surface cobalt. However, the color change could be an indication of nitride formation that proceeds too slowly to produce a visible compound at the lower reaction temperatures. No further characterizations were performed to identify the chemical composition of the species associated with the color change because the absence of NO activity did not justify further investigation and the  $\text{N}_2\text{O}$  decomposition rates did not appear to be affected by this structure or composition change. Color changes were not observed for the ceria catalysts in either the NO or  $\text{N}_2\text{O}$  decomposition experiments, although solid compounds of cobalt and ceria are reported as thermodynamically stable at these temperatures [16].

## N<sub>2</sub>O Decomposition

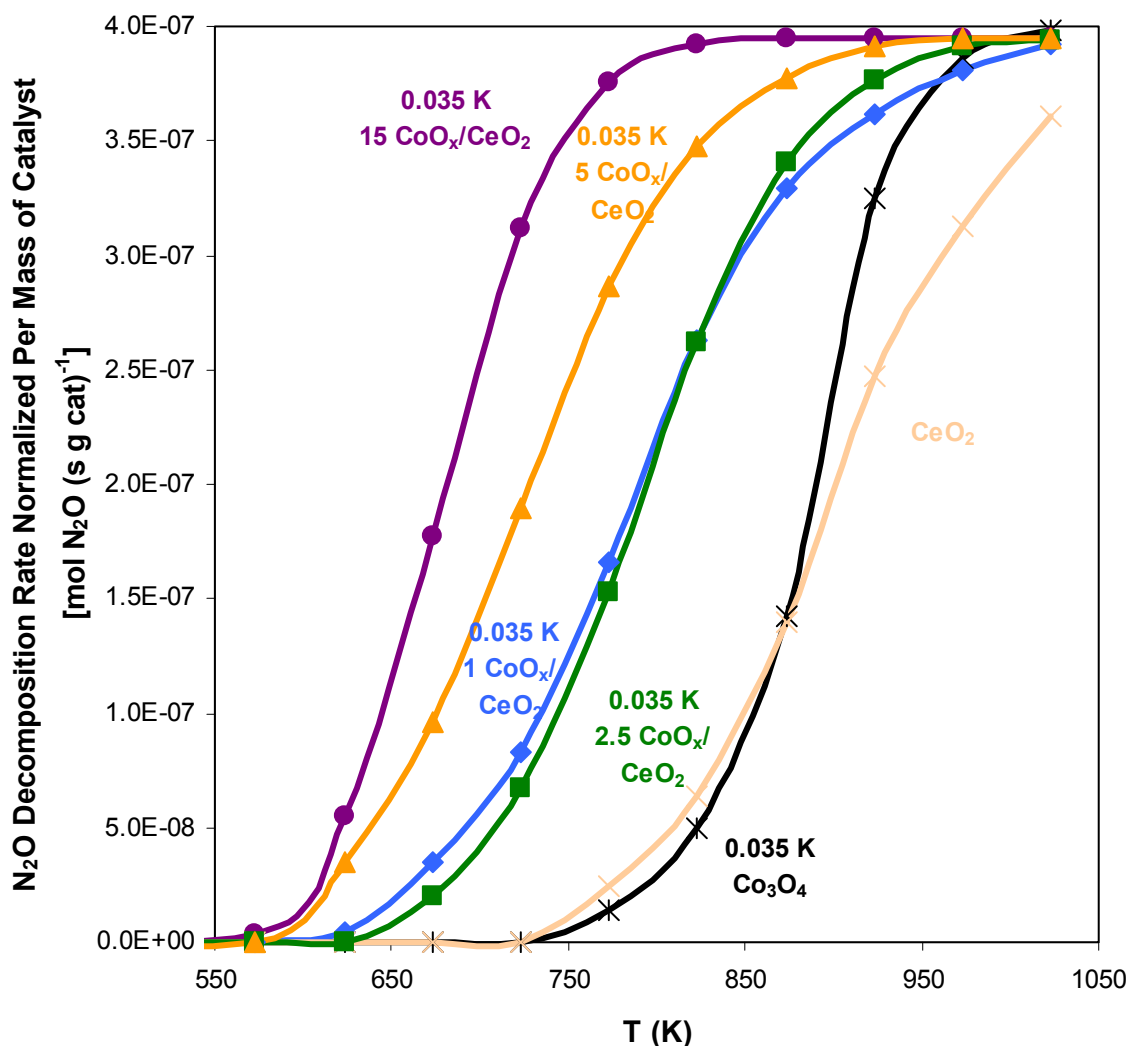
While the catalysts were not effective for NO decomposition, they had substantial N<sub>2</sub>O decomposition activity. N<sub>2</sub>O is typically present in much smaller quantities than NO in combustion gases, but it is more persistent in the atmosphere and is a stronger greenhouse gas [17]. Therefore, these catalysts could be useful for applications where N<sub>2</sub>O control is required, such as in nitric and adipic acid production processes, [17] or for combustion processes if more stringent environmental controls on N<sub>2</sub>O are required in the future.

Figure 5 shows the N<sub>2</sub>O conversion observed for several ceria-supported CoO<sub>x</sub> catalysts,



**Figure 5.** N<sub>2</sub>O conversion as a function of reaction temperature for a series of CoO<sub>x</sub>/CeO<sub>2</sub> catalysts with 0.035 K:Co. [0.6 cm<sup>3</sup>/s flow of 818 ppm N<sub>2</sub>O in N<sub>2</sub> and Ar; 0.04 g catalyst]

as well as for unsupported  $\text{Co}_3\text{O}_4$  and for ceria without cobalt. Figure 6 shows the same data in terms of the rate of  $\text{N}_2\text{O}$  decomposition normalized per mass of catalyst. All of the catalysts (except the ceria support, which has no cobalt) have potassium added in a 0.035 K:Co atomic ratio. All of  $\text{CoO}_x/\text{CeO}_2$  catalysts have significant activity between 573 and 773 K which is much greater than the activity of the unsupported  $\text{Co}_3\text{O}_4$  and the  $\text{CeO}_2$  over the same temperature range. The  $\text{CoO}_x/\text{CeO}_2$  catalysts clearly show a support effect because the combination catalysts



**Figure 6.**  $\text{N}_2\text{O}$  decomposition rate per mass of catalyst as a function of reaction temperature for a series of  $\text{CoO}_x/\text{CeO}_2$  catalyst with 0.035 K:Co atomic ratios. [ $0.6 \text{ cm}^3/\text{s}$  flow of 818 ppm  $\text{N}_2\text{O}$  in  $\text{N}_2$  and Ar;  $0.04 \text{ g}$  catalyst]

are much better than either of the two separate components. Interestingly,  $\text{CeO}_2$  alone is a better  $\text{N}_2\text{O}$  decomposition catalyst than unsupported  $\text{Co}_3\text{O}_4$  at lower reaction temperatures (673-873 K), but  $\text{Co}_3\text{O}_4$  is better at higher temperatures.

The supported catalysts with higher cobalt contents have higher reaction rates at a given temperature, with the order from highest to lowest of  $15 \text{ wt}\% \text{ CoO}_x/\text{CeO}_2 > 5 \text{ wt}\% \text{ CoO}_x/\text{CeO}_2 > 2.5 \text{ wt}\% \text{ CoO}_x/\text{CeO}_2 \cong 1 \text{ wt}\% \text{ CoO}_x/\text{CeO}_2$ , with the 2.5 wt%  $\text{CoO}_x$  catalyst having a slight rate advantage at higher temperatures and the 1 wt%  $\text{CoO}_x$  catalyst showing higher rates at lower temperatures. This order is inversely proportional to the edge energies shown in Figure 4, which suggests that the surface cobalt oxide sites with electronic characteristics more similar to bulk  $\text{Co}_3\text{O}_4$  are more active for  $\text{N}_2\text{O}$  decomposition. In Figure 6, the rates all reach the same asymptotic limit because the same amounts of catalyst were used in each experiment (0.04 g) and all catalysts (except  $\text{CeO}_2$ ) achieved 100% conversion of the  $\text{N}_2\text{O}$  at some point in the reaction temperature sequence (Figure 5).

The alumina-supported catalysts were all less effective at  $\text{N}_2\text{O}$  decomposition compared to the ceria-supported catalysts. As shown in Figure 7, all 0.035 K- $\text{CoO}_x/\text{Al}_2\text{O}_3$  catalysts converted over 90% of the  $\text{N}_2\text{O}$  fed to the reactor at 973 K, but this reaction temperature is 200 K higher than the best ceria-supported catalysts.  $\text{N}_2\text{O}$  conversion generally increased with increasing cobalt content of the catalysts, although the 2.5 wt% Co catalyst produced the highest conversions at temperatures above 873 K. In fact, the conversions achieved with the alumina-supported catalysts were not significantly better than unsupported  $\text{Co}_3\text{O}_4$  (the bold line in Figure 7) and were similar or worse above 923 K.

For comparison purposes, Figure 8 shows  $\text{N}_2\text{O}$  conversion as a function of temperature for both the ceria and alumina supported cobalt oxide catalysts with 0.035 K:Co. This figure

highlights the higher activity of the ceria-supported catalysts compared to the alumina-supported catalysts (at a given reaction temperature), despite the fact that the surface area of the ceria is approximately 1/10 that of the alumina ( $\sim 20 \text{ m}^2/\text{g}$  [14, 15] compared to  $\sim 200 \text{ m}^2/\text{g}$ ). The advantage of dispersing the cobalt oxide species over a much higher surface area was anticipated to increase reaction rates, but this expected result was not observed. Figure 8 also illustrates the higher reactor temperatures ( $\sim 200 \text{ K}$ ) required for the alumina-supported catalysts to achieve conversion similar to the ceria-supported catalysts.

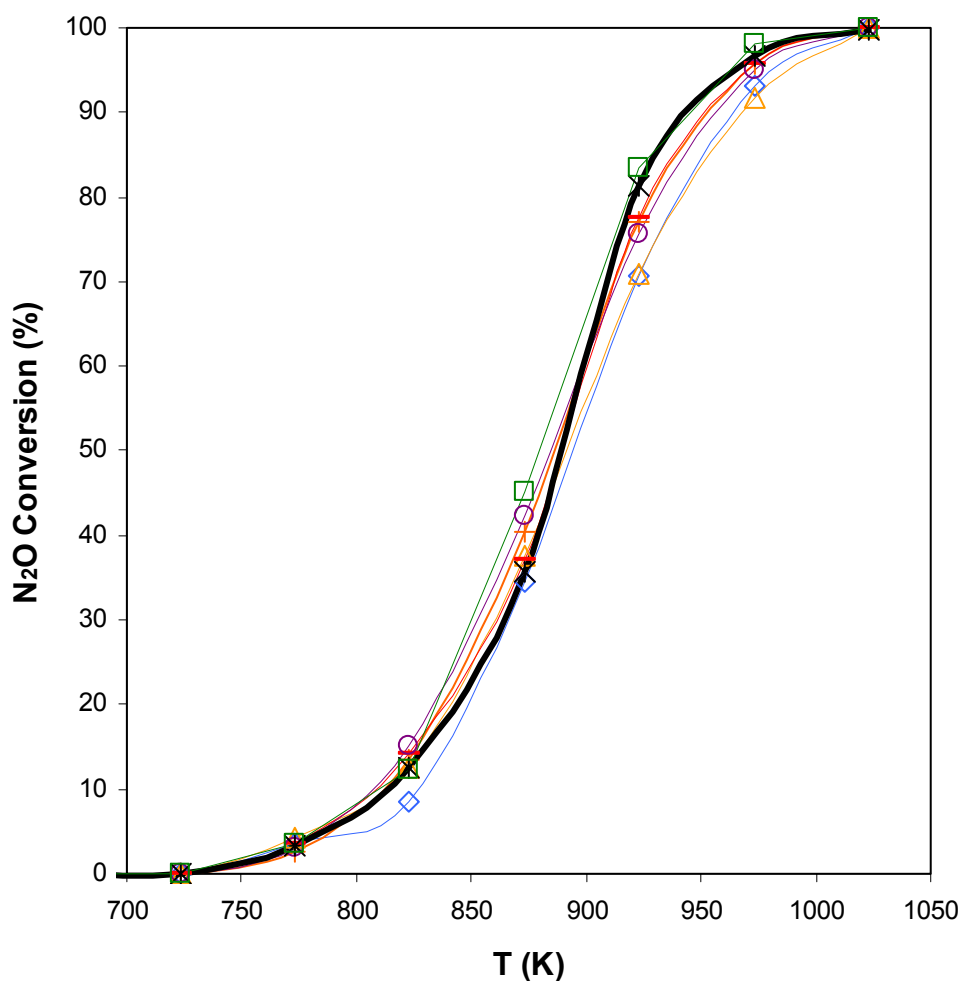


**Figure 7.**  $\text{N}_2\text{O}$  conversion as a function of reaction temperature for a series of 0.035 K- $\text{CoO}_x/\text{Al}_2\text{O}_3$  catalysts with varying amounts of Co. Diamond: 1 wt% Co; square: 2.5 wt% Co; triangle: 5.0 wt% Co; plus sign: 7.5 wt% Co; dash: 10 wt% Co; circle: 15 wt% Co. [ $0.6 \text{ cm}^3/\text{s}$  flow of 818 ppm  $\text{N}_2\text{O}$  in  $\text{N}_2$  and Ar; 0.04 g catalyst]

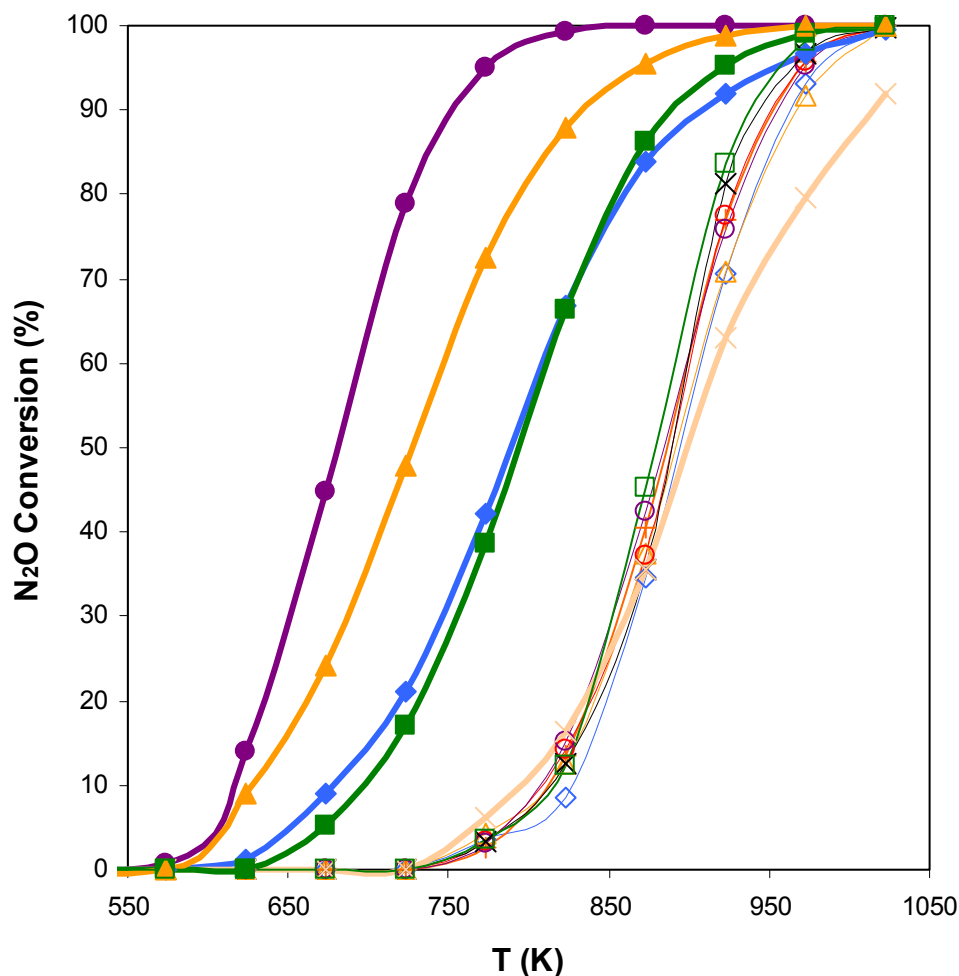


**Figure 8.** N<sub>2</sub>O conversion per mass of catalyst as a function of reaction temperature for a series of CoO<sub>x</sub>/CeO<sub>2</sub> and CoO<sub>x</sub>/Al<sub>2</sub>O<sub>3</sub> catalysts with 0.035 K:Co atomic ratios. Bold lines: ceria-supported catalysts and CeO<sub>2</sub> (legend in Figure 5); thin lines: alumina-supported catalysts (legend in Figure 7 caption). [0.6 cm<sup>3</sup>/s flow of 818 ppm N<sub>2</sub>O in N<sub>2</sub> and Ar; 0.04 g catalyst]

When the catalyst activity is reported on a nominal turnover frequency (TOF) basis (per mol of Co) as shown in Figure 9, the rates generally increase monotonically in activity with decreasing amount of cobalt (with the exception of the 2.5 and 5.0 wt% Co catalysts supported on ceria below 773 K). Figure 9a, which contains the TOF data for the ceria catalysts, and Figure 9b, which contains the TOF data for the alumina catalysts, have the same scales and again highlight the decreased activity of the cobalt on the alumina support. The catalysts with the lowest cobalt content (1 wt% CoO<sub>x</sub>/CeO<sub>2</sub> and 1.4 wt% CoO<sub>x</sub>/Al<sub>2</sub>O<sub>3</sub>) are most effective per cobalt

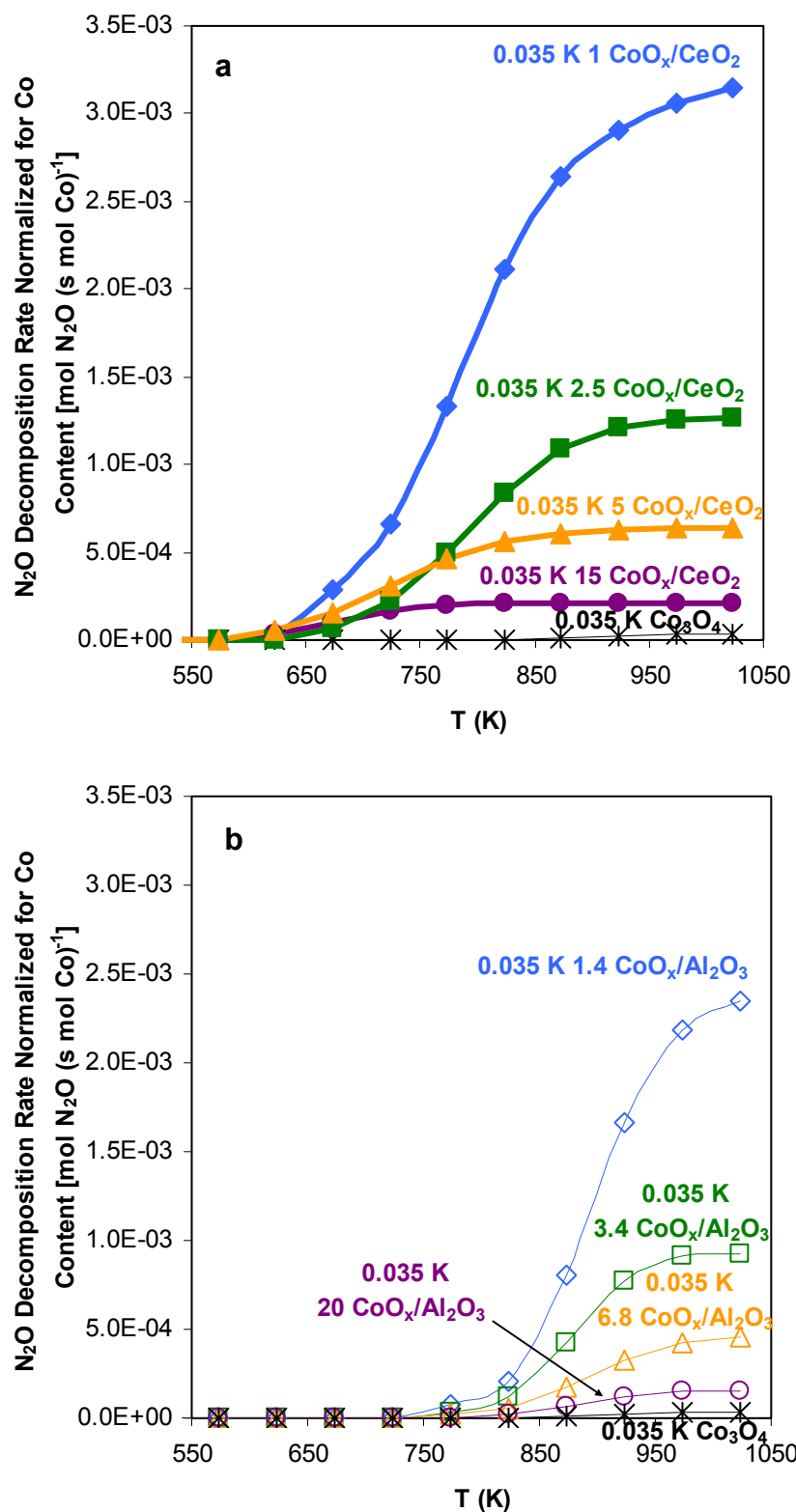


**Figure 9.** N<sub>2</sub>O decomposition rate normalized per mole of Co as a function of reaction temperature for the series of (a) CoO<sub>x</sub>/CeO<sub>2</sub> catalysts and (b) CoO<sub>x</sub>/Al<sub>2</sub>O<sub>3</sub> catalysts with 0.035 K:Co atomic ratios. [0.6 cm<sup>3</sup>/s flow of 818 ppm N<sub>2</sub>O in N<sub>2</sub> and Ar; 0.04 g catalyst]

atom because they have the highest number of cobalt oxide structures exposed on the surface. This result is consistent with more of the cobalt oxide being exposed and available for reaction on the catalysts with lower  $\text{CoO}_x$  contents, while the catalysts with higher  $\text{CoO}_x$  contents have fewer exposed surface  $\text{CoO}_x$  species available for reaction and more buried in bulk three-dimensional structures similar to crystalline  $\text{Co}_3\text{O}_4$  (as also suggested by the UV-visible edge energies in Figure 4). The TOF of the catalysts with the lowest cobalt content (1 wt%  $\text{Co}_3\text{O}_4/\text{CeO}_2$  and 1.4 wt%  $\text{Co}_3\text{O}_4/\text{Al}_2\text{O}_3$ ) are approximately an order of magnitude higher than the catalysts with the highest cobalt contents (15 wt%  $\text{Co}_3\text{O}_4/\text{CeO}_2$  and 20 wt%  $\text{Co}_3\text{O}_4/\text{Al}_2\text{O}_3$ ). This could be a result of inherent turnover frequency differences for the more dispersed cobalt species on the  $\sim 1.0$  wt% samples, but for the alumina-supported catalysts, it is more likely the result of some of the cobalt atoms being trapped in three dimensional crystal structures that are inaccessible for reaction, as mentioned above. The exposed surface cobalt oxide species in the ceria-supported catalysts with higher cobalt contents actually appear to be more active than the more dispersed species with higher edge energies found in the catalysts with lower cobalt oxide content (discussed in further detail in association with Tables 1 and 2, below).

In summary, the rate data in Figure 9, normalized for cobalt content, correlate with edge energies, shown in Figure 4, for the reasons discussed previously. The catalysts with lower cobalt content have UV-visible absorption higher edge energies associated with more dispersed cobalt oxide surface species that are more available for reaction and thus produce higher  $\text{N}_2\text{O}$  decomposition rates per cobalt, while those with lower edge energies are more like bulk  $\text{Co}_3\text{O}_4$  that have fewer surface cobalt oxide species and thus produce lower rates per cobalt. However, this effect appears to be counterbalance by an increase in intrinsic surface site activity for the ceria-supported catalysts with higher cobalt oxide contents.



In further summary, Tables 1 and 2 contain the N<sub>2</sub>O conversion rate data at 873 K reaction temperature, normalized for mass of catalyst and for number of Co atoms for the alumina and ceria-supported catalysts, respectively. The data in Table 1 show that the N<sub>2</sub>O decomposition rate per mass of catalyst is approximately constant for each of the alumina-supported catalysts. However, the catalysts with the highest rates per cobalt atom are the 1.4 wt% CoO<sub>x</sub>/Al<sub>2</sub>O<sub>3</sub> catalysts and the rates decrease with increasing cobalt oxide content.

Catalyst	N <sub>2</sub> O Decomposition Rate [x 10 <sup>-7</sup> mol/(s g catalyst)]	N <sub>2</sub> O Decomposition Rate [x 10 <sup>-4</sup> mol/(s mol Co)]
0.035 K- 1.4 CoO <sub>x</sub> /Al <sub>2</sub> O <sub>3</sub>	1.4	8.1
0.035 K- 3.4 CoO <sub>x</sub> /Al <sub>2</sub> O <sub>3</sub>	1.8	4.2
0.035 K- 6.8 CoO <sub>x</sub> /Al <sub>2</sub> O <sub>3</sub>	1.5	1.7
0.035 K- 10 CoO <sub>x</sub> /Al <sub>2</sub> O <sub>3</sub>	1.6	1.2
0.035 K- 14 CoO <sub>x</sub> /Al <sub>2</sub> O <sub>3</sub>	1.5	0.87
0.035 K- 20 CoO <sub>x</sub> /Al <sub>2</sub> O <sub>3</sub>	1.7	0.66
0.035 K – Co <sub>3</sub> O <sub>4</sub>	1.4	0.11

**Table 1.** N<sub>2</sub>O conversion rates normalized per mass of catalyst and for Co content for alumina-supported catalysts. [873 K, 0.6 cm<sup>3</sup>/s flow of 818 ppm N<sub>2</sub>O in N<sub>2</sub> and Ar; 0.04 g catalyst]

In contrast, the data in Table 2 show that the rates per mass of catalyst increase with increasing cobalt content for the ceria-supported catalysts. As mentioned previously, this rate effect is attributable to a support effect because the interaction of the cobalt oxide and ceria produce rates of N<sub>2</sub>O decomposition that are 2-3 times larger than either the Co<sub>3</sub>O<sub>4</sub> or the ceria when normalized per catalyst mass. As with the alumina-supported catalysts shown in

Catalyst	N <sub>2</sub> O Decomposition Rate [x 10 <sup>-7</sup> mol/(s g catalyst)]	N <sub>2</sub> O Decomposition Rate [x 10 <sup>-4</sup> mol/(s mol Co)]
0.035 K- 1.0 CoO <sub>x</sub> /CeO <sub>2</sub>	3.3	27
0.035 K- 2.5 CoO <sub>x</sub> /CeO <sub>2</sub>	3.4	11
0.035 K- 5.0 CoO <sub>x</sub> /CeO <sub>2</sub>	3.8	6.1
0.035 K- 15 CoO <sub>x</sub> /CeO <sub>2</sub>	4.0	2.1
CeO <sub>2</sub>	1.4	–

**Table 2.** N<sub>2</sub>O conversion rates normalized per mass of catalyst and for Co content for ceria-supported catalysts. [873 K, 0.6 cm<sup>3</sup>/s flow of 818 ppm N<sub>2</sub>O in N<sub>2</sub> and Ar; 0.04 g catalyst]

Table 1, the decreasing rate per cobalt atom with increasing cobalt oxide content has been explained earlier as a consequence of fewer cobalt oxide species remaining on the surface and available for reaction. However, the increasing rate per catalyst mass with increasing cobalt oxide content for the ceria-supported catalysts strengthens the argument that the intrinsic activity of the surface species is increasing as these surface domains acquire more  $\text{Co}_3\text{O}_4$  character (as shown by the absorption edge energy data in Figure 4).

Rates of  $\text{N}_2\text{O}$  decomposition on the ceria-supported catalysts are also 2-3 times higher than those on the alumina-supported catalysts with similar cobalt oxide contents. This direct comparison is somewhat misleading because the ceria-supported catalysts achieved much higher  $\text{N}_2\text{O}$  conversions (80-100%) relative to the alumina-supported catalysts (~40%) at this temperature. For reactions with positive order rate dependencies, the rate slows with decreasing concentration (corresponding to increasing conversion). Thus, if the rates were compared at equal conversions at this temperature, the relative rate difference between the ceria and alumina-supported catalysts would be even greater.

### **Alkali Addition**

Based on previous reports on unsupported  $\text{Co}_3\text{O}_4$ , the highest NO decomposition rates were observed for catalysts with 0.035 K:Co atom ratios [8]. Therefore, the majority of the catalysts in this study were prepared with added alkali. All of the alumina catalysts were tested with three amounts of K, including 0.01, 0.035, and 0.05 K:Co atom ratio. However, a series of the alumina supported catalysts were prepared without added alkali and were tested for  $\text{N}_2\text{O}$  decomposition. Potassium generally reduced  $\text{N}_2\text{O}$  conversion rates, with the effect becoming more severe with increasing K content. In all cases, the catalysts with no potassium produced the highest rates. A typical catalyst series that demonstrates the negative impact of K on  $\text{N}_2\text{O}$

decomposition rates is shown in Figure 10 for the 2.5 wt% Co/Al<sub>2</sub>O<sub>3</sub> (3.4 wt% CoO<sub>x</sub>/Al<sub>2</sub>O<sub>3</sub>) catalysts. The data points at 873 K most clearly demonstrate the decrease in conversion (which is proportional to rate) with increasing K content. These data are highlighted in Table 3, which shows the decrease in conversion rate, normalized per mass of catalyst and per cobalt atom with increasing K content for this catalyst at 873 K. The rate decreases by ~50% between the catalyst with no added potassium compared to the one with 0.05 K:Co. These trends were generally followed for catalysts with different cobalt oxide loadings and with other alkali metal oxides.

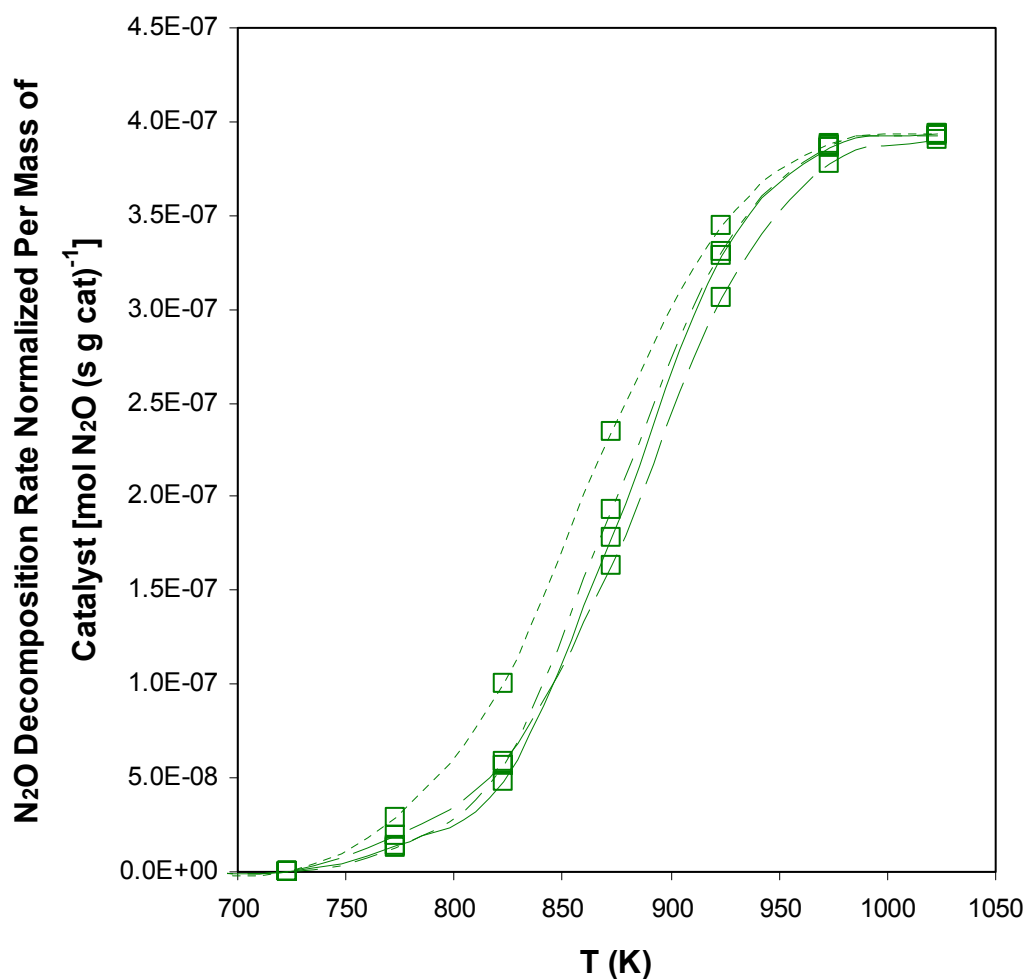


Figure 10. N<sub>2</sub>O decomposition rate normalized per weight of catalyst as a function of reaction temperature for a 3.4 wt% CoO<sub>x</sub>/Al<sub>2</sub>O<sub>3</sub> catalyst with varying amounts of potassium. Dotted line: no added K; short dashed line: 0.01 K:Co; solid line: 0.035 K:Co; long dashed line: 0.05 K:Co. [0.6 cm<sup>3</sup>/s flow of 818 ppm N<sub>2</sub>O in N<sub>2</sub> and Ar; 0.04 g catalyst]

Catalyst	N <sub>2</sub> O Decomposition Rate [x 10 <sup>-7</sup> mol/(s g catalyst)]	N <sub>2</sub> O Decomposition Rate [x 10 <sup>-4</sup> mol/(s mol Co)]
0 K – 3.4 CoO <sub>x</sub> /Al <sub>2</sub> O <sub>3</sub>	2.3	5.5
0.01 K – 3.4 CoO <sub>x</sub> /Al <sub>2</sub> O <sub>3</sub>	1.9	4.6
0.035 K – 3.4 CoO <sub>x</sub> /Al <sub>2</sub> O <sub>3</sub>	1.8	4.2
0.05 K – 3.4 CoO <sub>x</sub> /Al <sub>2</sub> O <sub>3</sub>	1.6	3.8

**Table 3.** N<sub>2</sub>O conversion rates normalized per mass of catalyst and for Co content for the 2.5 wt% Co/Al<sub>2</sub>O<sub>3</sub> (3.4 wt% CoO<sub>x</sub>/Al<sub>2</sub>O<sub>3</sub>) catalysts showing typical effects of K addition. [873 K, 0.6 cm<sup>3</sup>/s flow of 818 ppm N<sub>2</sub>O in N<sub>2</sub> and Ar; 0.04 g catalyst]

This behavior is quite different from the effect of alkali oxide content observed by Haneda *et al.* [8] for NO decomposition on the unsupported Co catalyst. They observed maximum rates for intermediate alkali metal contents with about 0.035 A:Co ratios, with K being the most beneficial. The explanation for this difference between our results and those reported by Haneda *et al.* may simply be that N<sub>2</sub>O requires different surface properties or follows a different reaction mechanism that are favored without the presence of alkali metal oxides compared to NO.

## CONCLUSION

The cobalt oxide catalysts supported on Al<sub>2</sub>O<sub>3</sub> and CeO<sub>2</sub> show appreciable rates of N<sub>2</sub>O decomposition, but not NO decomposition. The CeO<sub>2</sub>-supported catalysts have much higher N<sub>2</sub>O decomposition rates at a given reaction temperature compared to the Al<sub>2</sub>O<sub>3</sub>-supported catalysts and thus are able to produce similar rates at 200 K lower reaction temperatures. The trend of increasing rate per cobalt atom with decreasing cobalt content correlates to increasing edge energies measured by UV-visible spectroscopy. This trend relates both to higher accessibility of the cobalt oxide structures on the surface of the catalysts with lower cobalt oxide contents and, for the ceria-supported catalysts, to higher intrinsic activity of the cobalt oxide surface species with higher cobalt oxide content. One of the CeO<sub>2</sub>-supported catalysts (15 wt%

CoO<sub>x</sub> or 11 wt% Co) achieved over 90% N<sub>2</sub>O decomposition at 673 K and the other reaction conditions in this study. This activity could be enhanced at lower reaction temperatures by reducing the space velocity within the reactor, either by reducing the flow rate or increasing the amount of catalyst. Such a catalyst might be suitable for the commercial N<sub>2</sub>O abatement applications as an alternative to more expensive metal-based catalysts [17].

## REFERENCES

1. G. Centi, S. Perathoner, F. Vazzana, M. Marella, M. Tomaselli, M. Mantegazza, *Environ. Res.* **4** (2000) 325.
2. H. Bosch, F. Janssen, *Catal. Today* **2** (1988) 369.
3. V. I. Parvulescu, P. Grange, B. Delmon, *Catal. Today* **46** (1998) 233.
4. G. Busca, L. Lietti, G. Ramis, F. Berti, *Appl. Catal. B* **18** (1988) 1.
5. J. M. Thomas, W. J. Thomas, *Principles and Practice of Heterogeneous Catalysis* VHC, Weinheim, Germany 1997 578.
6. M. Shelef, K. Otto, H. Gandhi, *Atmos. Environ.* **3** (1969) 107.
7. A. Amirnazmi, M. Boudart, *J. Catal.* **39** (1975) 383.
8. M. Haneda, Y. Kintaichi, N. Bion, H. Hamada, *Appl. Catal. B* **46** (2003) 473.
9. G. K. Boreskov, *Discuss. Faraday Soc.* **41** (1966) 263.
10. L. F. Liotta, G. Pantaleo, A. Macaluso, G. Di Carlo, G. Deganello, *Appl. Catal. A* **245** (2003) 167.
11. Ch. Papadopoulou, J. Vakros, H. K. Matralis, C. Kordulis, A. Lycourghiotis, *J. Colloid Interface Sci.* **261** (2003) 146.
12. M. D. Argyle, Ph.D. Dissertation, University of California at Berkeley, 2003.
13. B. T. Kilbourn, *Cerium: A Guide to its Role in Chemical Technology* Molycorp, Mountain Pass, CA, 1992.
14. M. Kang, M. W. Song, K. L. Kim, *React. Kinet. Catal. Lett.* **79** (2003) 3-10.
15. M. Kang, M. W. Song, C. H. Lee, *Appl. Catal. A* **251** (2003) 143-156.
16. S. S. Kim, *J. Alloys and Compounds* **390** (2005) 223-225.
17. F. Kapteijn, J. Rodriguez-Mirasol, J. A. Moulijn, *Appl. Catal. B* **9** (1996) 25-64.